GA-C19465
3/91

HIGH-TEMPERATURE CERAMIC SUPERCONDUCTORS

FOR PERIOD
OCTOBER 1, 1990 TO MARCH 31, 1991

Prepared for
OFFICE OF NAVAL RESEARCH
800 NORTH QUINCY STREET
ARLINGTON, VIRGINIA 22217-5000

DARPA/ONR CONTRACT N00014-88-C-0714

APPROVED FOR PUBLIC RELEASE

Prepared by
K.S. MAZDIYASNI, PROGRAM MANAGER

K.C. CHEN
M.B. MAPLE (UCSD)
L. PAULIUS (UCSD)
P.K. TSAI (UCSD)

GA PROJECT 3850

APPROVED BY: T.D. Gulden
T.D. GULDEN
DIRECTOR, DEFENSE MATERIALS

GENERAL ATOMICS

CONTENTS

FIGURES

TABLES

1. INTRODUCTION

This is the sixth and seventh quarterly progress report on the work performed in the period from October 1, 1990 through March 31, 1991 on Office and Naval Research (ONR) Contract N00014-88-C-0714, entitled "High-Temperature Ceramic Superconductors." The principal objectives of this program are (1) to demonstrate fabrication of high-temperature ceramic superconductors that can operate at or above 90 K with appropriate current density, J_c, in forms useful for application in resonant cavities, magnets, motors, sensors, computers, and other devices; and (2) to fabricate and demonstrate selected components made of these materials, including microwave cavities and magnetic shields.

1.1. PROJECT OUTLINE

This program consists of six tasks: (1) metal alkoxide synthesis and processing, (2) microstructural evaluation and property measurement, (3) electrical and magnetic property measurement, (4) superconductor ceramic processing, (5) component fabrication and demonstration, and (6) reporting.

Task 1 is to synthesize a homogeneous alkoxide solution that contains all the constituent elements that can be easily made into powders, thin film, or drawn into fiber form. Ideally, this solution should possess precise stoichiometry, adequate stability, polymerizability, adherence, and spinnability. Also, the polymeric materials formed from this solution should be thermosetting, be able to be dissolved in organic solvents, and contain as little as possible low-temperature pyrolyzable organics with high char yield.

Task 2 is to study the microstructure as a function of processing parameters. The study includes: density, pore size and pore size distribution, phase identification, chemical composition and purity, environmental stability, effects of heat treatment, residual strain, seeding, annealing in magnetic fields, and epitaxy on grain growth and orientation.

Task 3 is to study the electrical and magnetic properties of the $YBa_2Cu_3O_7$ (123) high T_c ceramic superconductors. It will include both the ac electrical resistance (R_{ax}) and the ac magnetic susceptibility (χ_{ac}).

Task 4 is to investigate superconductor ceramic processing. Most of the important applications of superconductors require material in the form of fiber or films. Magnets, conductors, motors, and generators are examples of applications employing fiber; while detectors, microwave cavities, and microcircuitry require superconducting material in the form of films. The sol-gel process is ideally suited to producing materials in these forms; in fact, it is used commercially to produce antireflection and mirror coatings and to produce continuous ceramic fibers for structural reinforcement in composite materials and for thermal insulation.

Originally Task 5 was to demonstrate component fabrication. GA under the original SWO had to design and build a high Q, high T_c superconducting cavity using its unique sol-gel coating process capabilities. This task would have proceeded after some initial coating tests verified dc superconductivity and questions of adhesiveness, surface preparation, and processing procedures were answered. As the fabrication process and the materials quality were improved throughout the three-year program, two additional cavities would have been constructed and tested. Coupling would have been through a waveguide inductive iris into an end wall with a logarithmic decrement technique of Q measurement were considered most appropriate for the high Q anticipated. An X-band (10 GHz)

frequency choice allows for convenient dimensions of 4.3 cm diameter by 2.8 cm height. However, DARPA/ONR recent recommendation to General Atomics (GA) was to curtail the work on the cavity and concentrate on improving the quality and transport properties of solution condensed films activity.

Management Problem

Since the authorized funds for the program was exhausted by late October 1990, technical work was cut to a minimum rate of effort at GA's risk to keep the program going until FY-91 funds for the program was made available. The lack of funds during this time will neither affect the cost or the work schedule under the subject program. This report will focus primarily on Tasks 3 and 4.

1.2. MELT TEXTURING OF SOL-GEL DERIVED FIBERS

Equipment: Infrared Furnace Design and Construction

In this period the activity under the subject contract was mainly concentrated in the design, construction, and calibration of the commercially available infrared furnace for melt texturing purpose shown in Fig. 1. Also preliminary experiments were carried out on melt texturing of sol-gel derived YBCO (123) high T_c superconductor fibers. Some of the advantages of using infrared furnace for the purpose indicated are: (1) very rapid heating rates, room temperature to 1100°C in approximately 20 s; (2) the heating and cooling may be controlled very precisely and within the range $\leq \pm 1$°C for an extended period of time; (3) the radiation can be focused into a line; (4) create a steep yet controllable heat gradient along a length of fiber sample; and (5) it is highly efficient and simple equipment to operate.

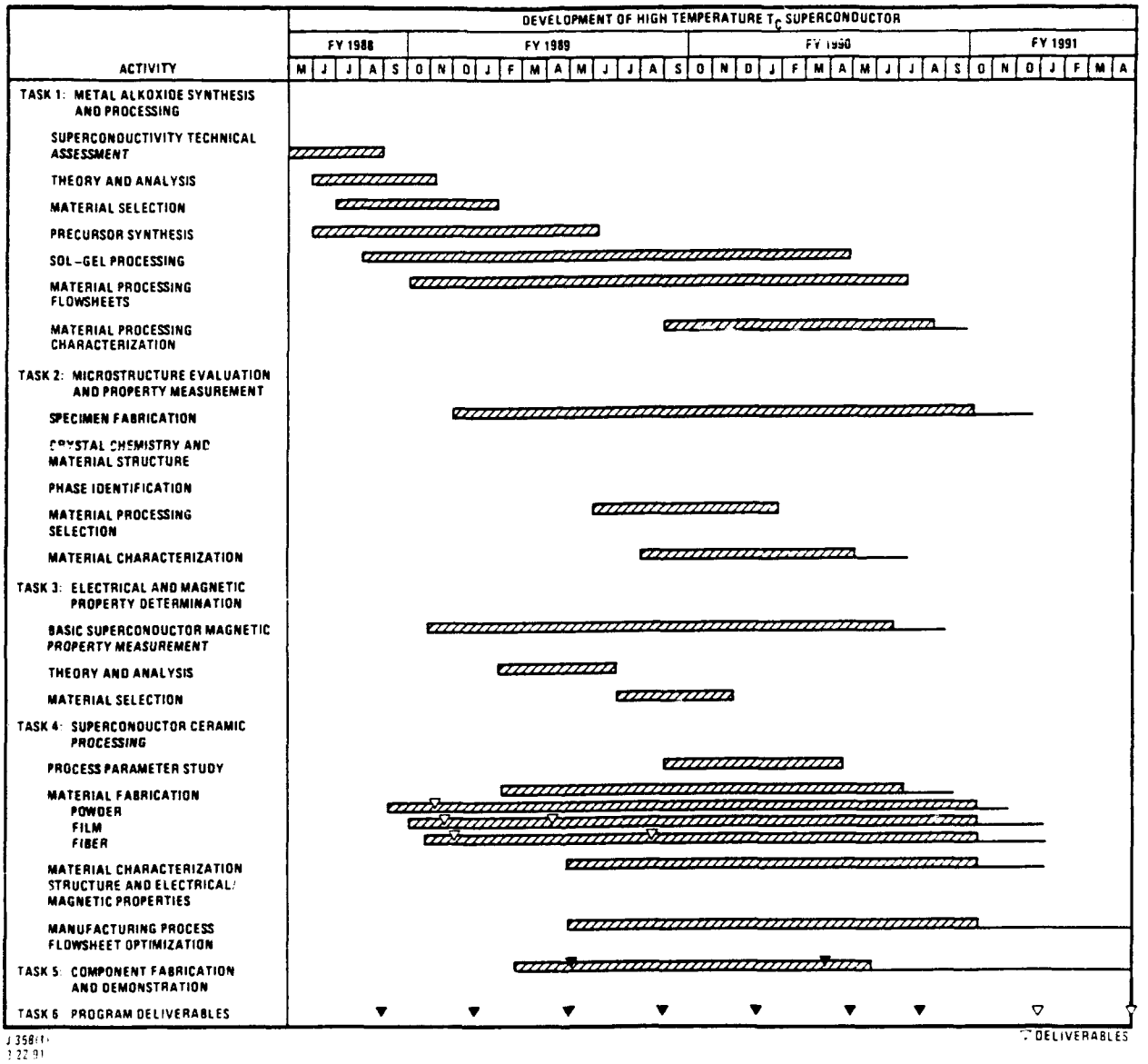
DEVELOPMENT OF HIGH TEMPERATURE T_c SUPERCONDUCTOR
FY 1988
FY 1989
FY 1990
FY 1991
M J J A S O N D J F M A M J J A S O N D J F M A M J J A S O N D J F M A
ACTIVITY
TASK 1: METAL ALKOXIDE SYNTHESIS AND PROCESSING
SUPERCONDUCTIVITY TECHNICAL ASSESSMENT
THEORY AND ANALYSIS
MATERIAL SELECTION
PRECURSOR SYNTHESIS
SOL-GEL PROCESSING
MATERIAL PROCESSING FLOWSHEETS
MATERIAL PROCESSING CHARACTERIZATION
TASK 2: MICROSTRUCTURE EVALUATION AND PROPERTY MEASUREMENT
SPECIMEN FABRICATION
CRYSTAL CHEMISTRY AND MATERIAL STRUCTURE
PHASE IDENTIFICATION
MATERIAL PROCESSING SELECTION
MATERIAL CHARACTERIZATION
TASK 3: ELECTRICAL AND MAGNETIC PROPERTY DETERMINATION
BASIC SUPERCONDUCTOR MAGNETIC PROPERTY MEASUREMENT
THEORY AND ANALYSIS
MATERIAL SELECTION
TASK 4: SUPERCONDUCTOR CERAMIC PROCESSING
PROCESS PARAMETER STUDY
MATERIAL FABRICATION
POWDER
FILM
FIBER
MATERIAL CHARACTERIZATION STRUCTURE AND ELECTRICAL/ MAGNETIC PROPERTIES
MANUFACTURING PROCESS FLOWSHEET OPTIMIZATION
TASK 5: COMPONENT FABRICATION AND DEMONSTRATION
TASK 6: PROGRAM DELIVERABLES
DELIVERABLES

MILESTONE

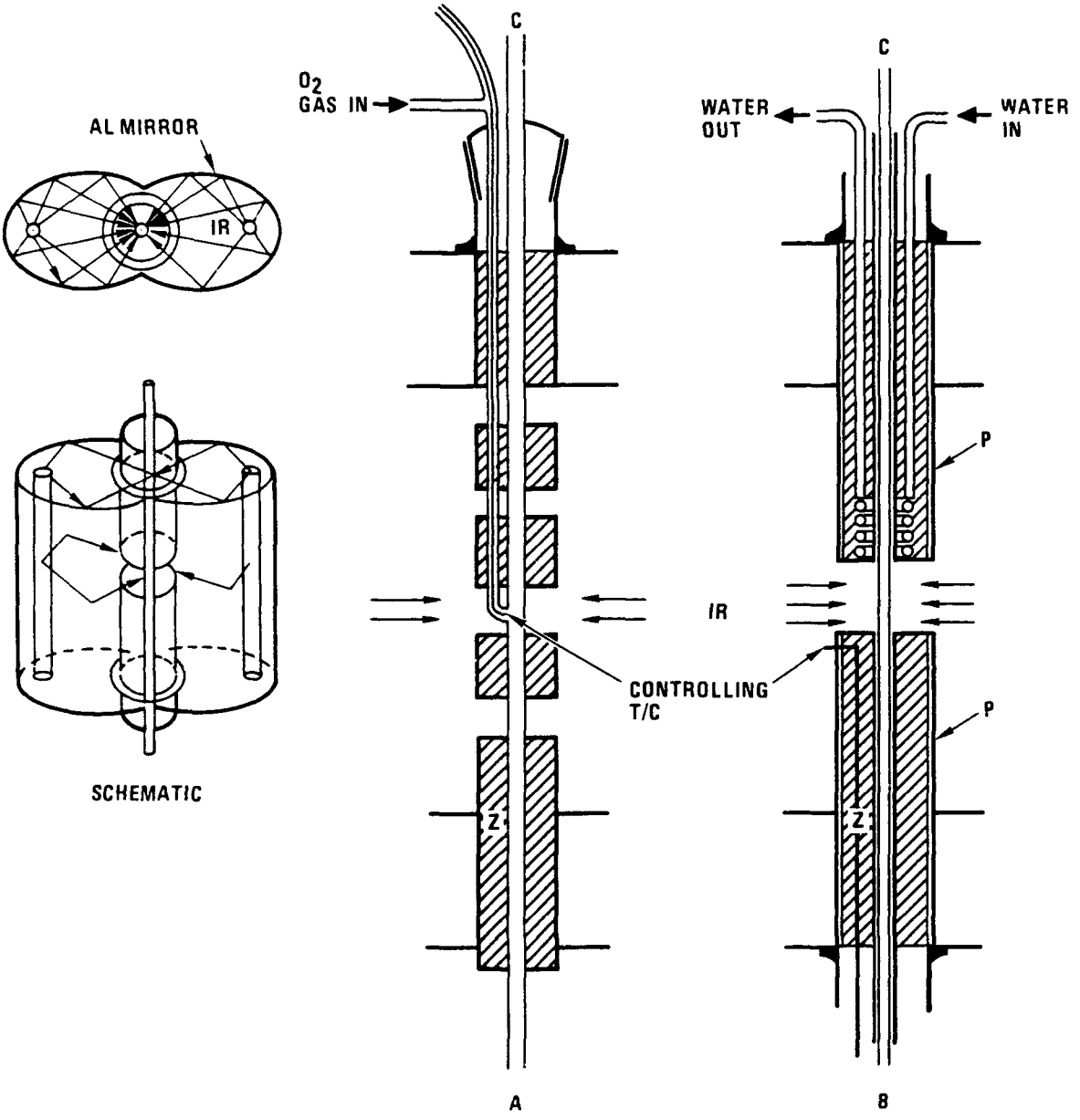

Fig. 1. (a) Infrared furnace with thermal gradient for melt-texturing; (b) modified infrared furnace for melt-texturing. C: central quartz tube; Z: Zircar block; P: platinum reflector

Test Samples Assembly

Utilizing the aforementioned characteristics of such a furnace, short samples of sol-gel derived small diameter 0.5 mm by 5 cm long extruded and sintered 123 rods to be melt textured were positioned at the center of quartz tube and travelled up and down by a slow speed motor at a constant speed. By insulating segments of quartz tubing, shown in Fig. 1, it was possible to increase the fiber throughput for melt texturing.

Furnace Modification

Unexpected problems were encountered in this first temperature gradient design [Fig. 1(a)]. It was found that during the rapid ramping of the infrared furnace, the aluminum reflective surface used for focusing the infrared radiation was rapidly corroded by the evaporated water vapor trapped inside the ceramic insulation Zircar blocks used to block portions of infrared radiation. Also, during the melt-texturing, the quartz tube was stained or corroded by the vapor species coming out from both of the travelling thermal couple and the Y123 sample and rapid loss of its transparency to infrared radiation after only a few test runs. The maximum thermal gradient had an initial value of 20°C/mm but this gradient decreased after several runs. In order to eventually adapt this furnace to continuous fiber texturing process, major modification of the furnace design had to be made, specifically in the radiation blocking arrangement.

In the redesigned furnace [Fig. 1(b)], all the Zircar insulation blocks were enclosed within two close-ended quartz cylinders to avoid water corrosion of the aluminum reflector surface. The central quartz tube could be replaced, as needed, to maintain transparency to the infrared radiation. In addition, a water-cooled copper coil was introduced to create even greater thermal gradient. Also, the controlling thermocouple was inserted away from the focal line of the infrared

radiation and calibrated. The temperature and the thermal gradient along the infrared focal line was measured after the temperature at the controlling thermocouple stabilized at 950°C. The sample temperature was monitored by a travelling thermocouple which was attached to the sample by a platinum wire. With this furnace modification it was possible to achieve a temperature gradient of 42°C/mm, schematically shown in Fig. 2, in the temperature range of 920° to 960°C.

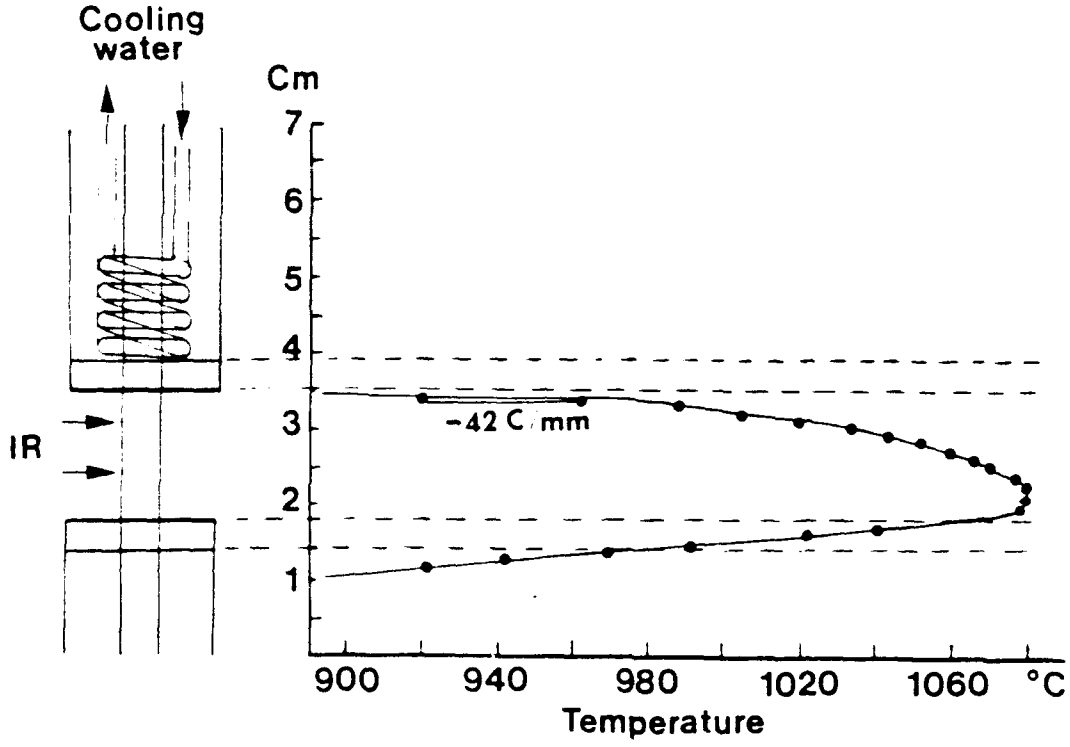

Fig. 2. Thermal gradient of the modified infrared furnace in Fig. 1(b)

2. MELT-TEXTURING OF SMALL DIAMETER Y123 RODS

The texturing experiment was first carried out on the Y123 rods of 0.5 mm to 0.9 mm in diameter and 5 cm long. The objectives of the experiment were to optimize the effects of maximum temperature, temperature gradient, traveling speeds, and the sample dimension (diameter) on melt texturing. The first series of the samples were processed in a constant temperature using different up-drawing speeds to study the resultant microstructure. The up-drawing speed and the maximum processing temperature of the Y123 samples are listed in Table 1. Their corresponding microstructures are also shown in Figs. 3 through 9. However, due to the loss of transparency in the centered quartz tube, the maximum temperature that samples was exposed to was decreased from 1080° to 1000°C even though the temperature of the controlling thermocouple was kept at 950°C.

In the first experiment, a 0.9 mm diameter extruded rod (10105-EX-H69-MT1) was pulled upward through the infrared furnace. The polarized optical micrograph on the polished section along the length of the Y123 rod indicates some degree of the preferred orientation has been achieved after the melt-texture process. The grain size is approximately 30 to 50 microns. However, it is seen that the preferred orientation does not always occur in the most desirable direction, i.e., with c axes of the grain parallel to the rod axis. There are several possible reasons for this angular inclination to occur. One possible reason is that the thermal gradient is not large enough. Another reason being variable loss of transparency in the central quartz tube resulting in nonuniform infrared intensity at the fiber surface. Yet another reason might be due to the rod not being perfectly straight so that when it traveled along the quartz tube, it was not at the center of

TABLE 1
PRELIMINARY PROCESS PARAMETERS OF MELT-TEXTURED
SOL-GEL DERIVED YBCO FIBERS

Sample Size (mm)	Traveling Speed (cm/min)	Maximum Temperature (°C)	Zones
10105-EX-H69-MT1[a]	0.0208	1080	3
10377-EX-MT2[a]	0.0269	947	1
10377-15B-MT3	0.0325	1078	3
10377-15B-MT4	0.0589		2
10377-15B-MT5	0.0590	960	2
10377-15B-MT6	0.0610	1006	2
10377-15B-MT7	0.0267	1010	2
10377-15B-MT8	0.0267	1000	2
10377-15B-MT9	0.0288	1005	2

[a]Diameter = 0.9 mm; others 0.5 mm in diameter.

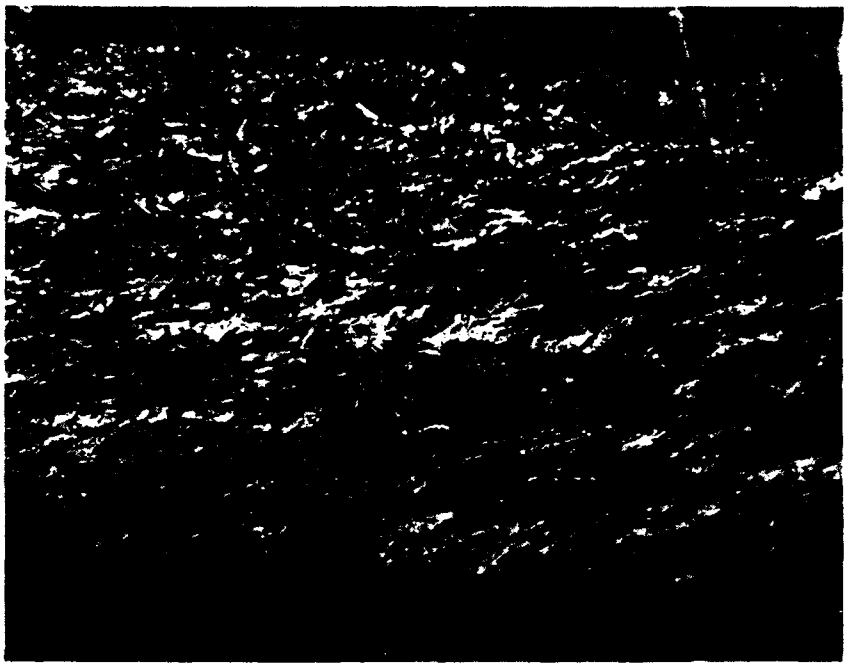

Fig. 3(a). Optical micrograph of the melt-textured sample 10105-EX-H69-MT1 in polarized light showing partial alignment along the axial direction (100X)

Fig. 3(b). Optical micrograph of the same sample under unpolarized light showing alignment with remaining porosity (100X)

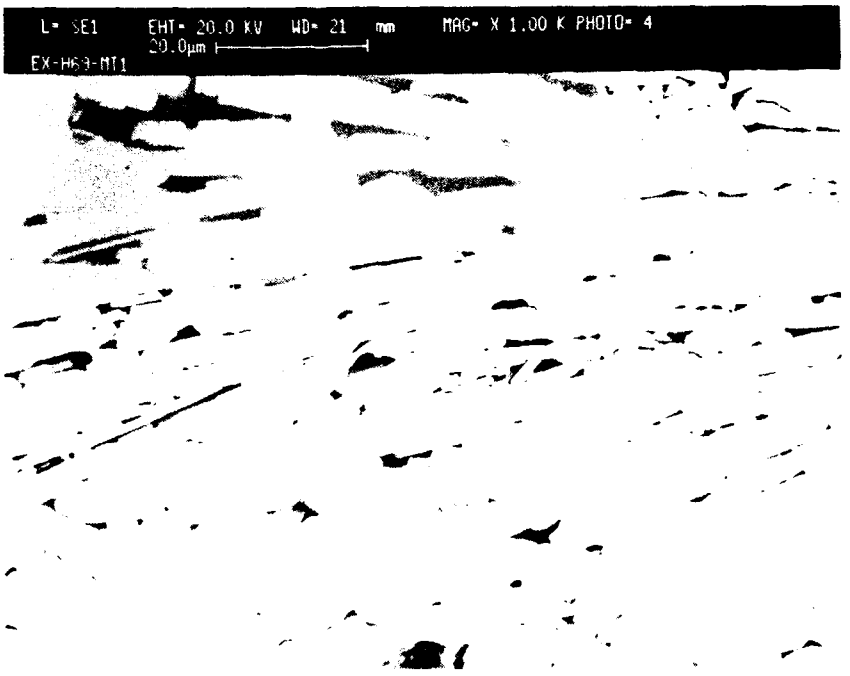

Fig. 3(c). SEM micrograph of enlarged section of Fig. 3(b) to show the alignment as well as porosity (1000X)

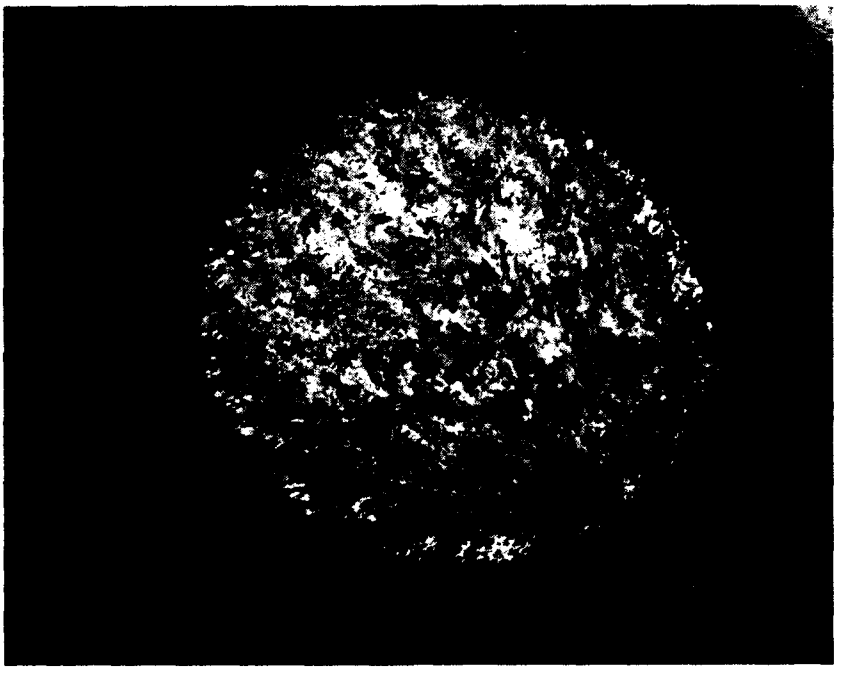

Fig. 3(d). The polished cross section of the melt-textured sample MT001 shows the alignment with an oblique angle to the fiber axis (100X)

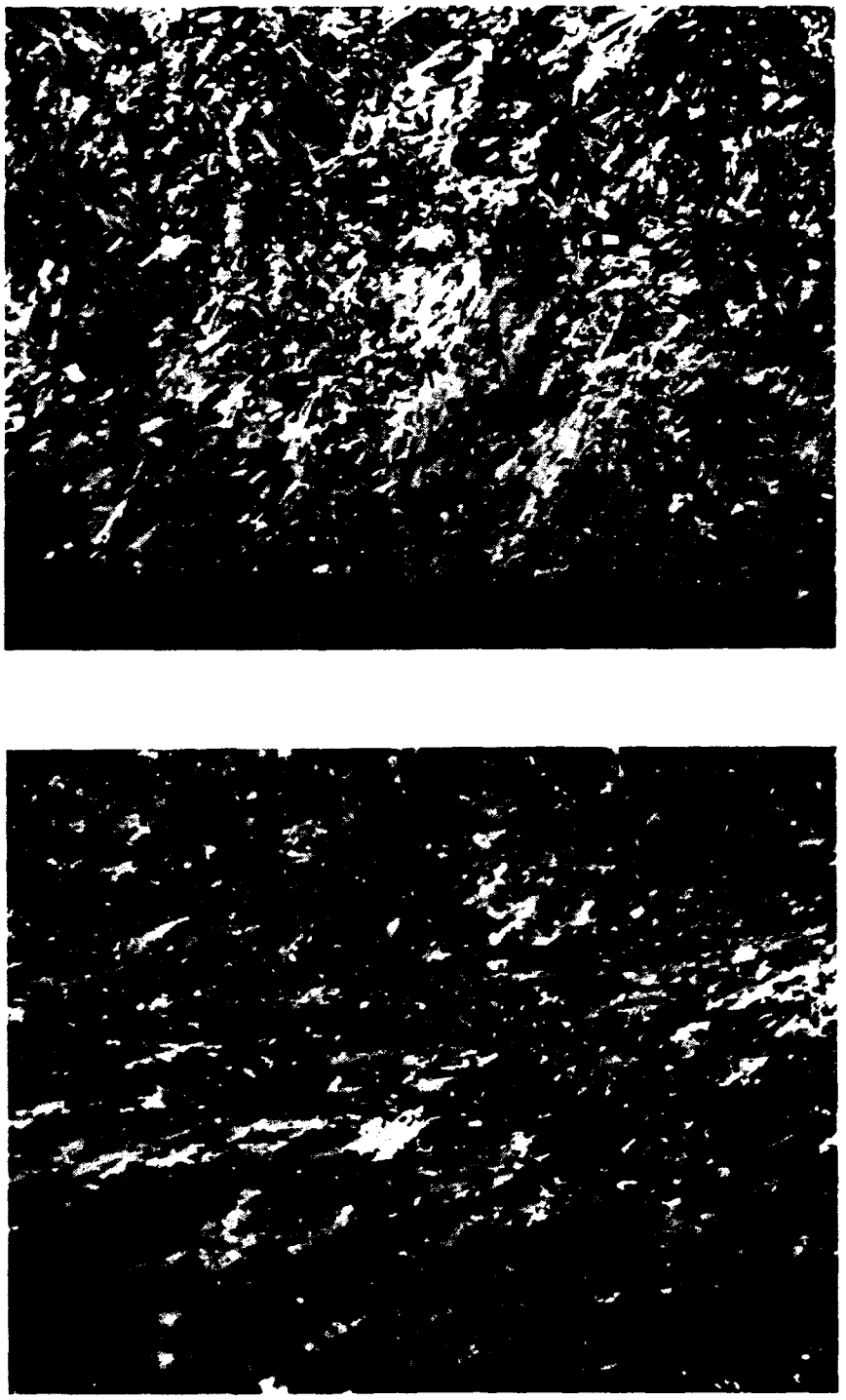

Fig. 4. Polarized light microstructure of two melt-textured longitudinal sections showing partial alignment (200X)

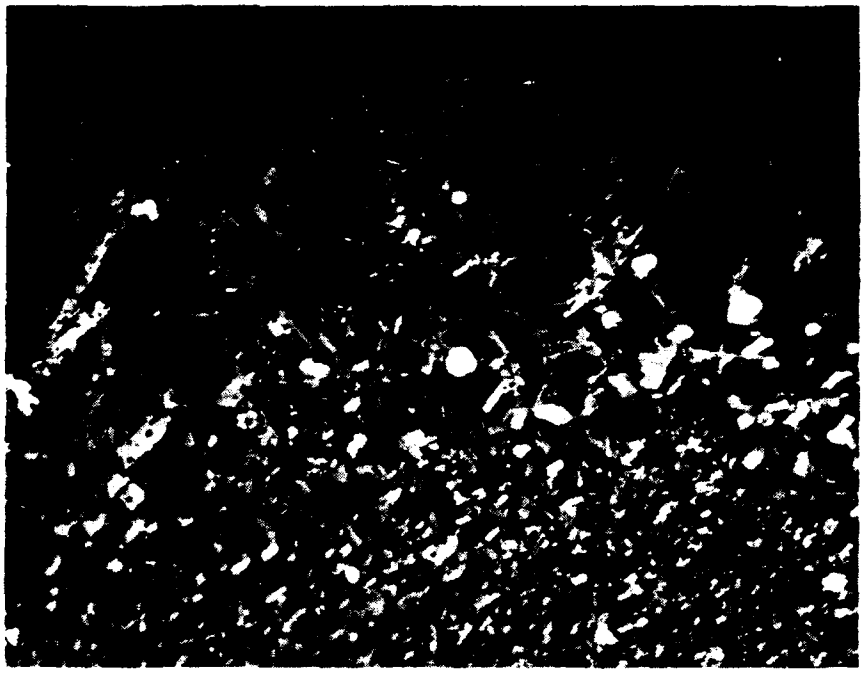

Fig. 5. The melt-textured longitudinal section of sample 10337-15B MT4 in polarized light showing the nonuniform melt-texturing that may be due to the fiber being off-center in the furnace or loss of transparency in the central quartz tube (200X)

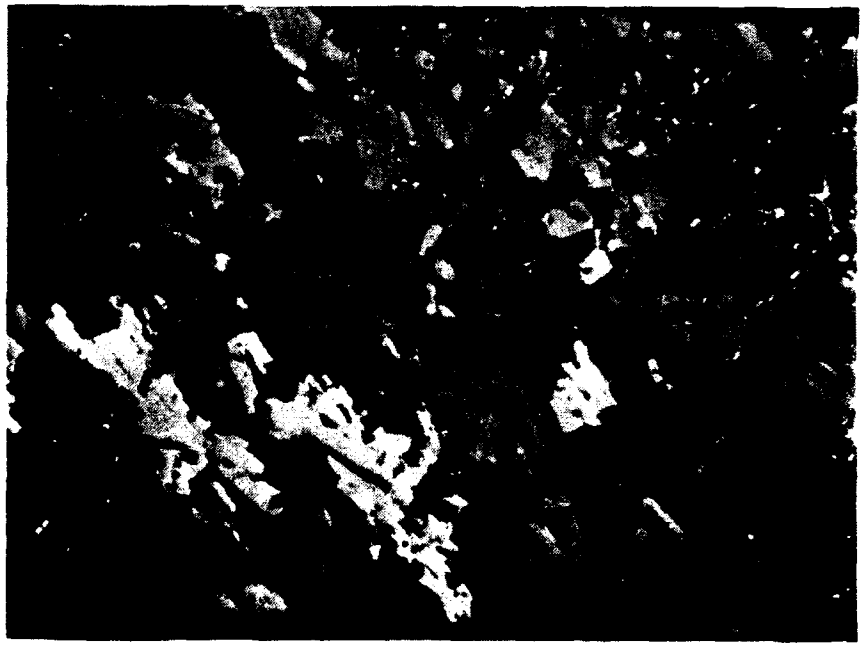

Fig. 6. The melt-textured longitudinal section of sample 10337-15B MT5 in polarized light showing excessive grain growth due to the loss of transparency in the quartz tube lowering the maximum attainable temperature to 960°C (200X)

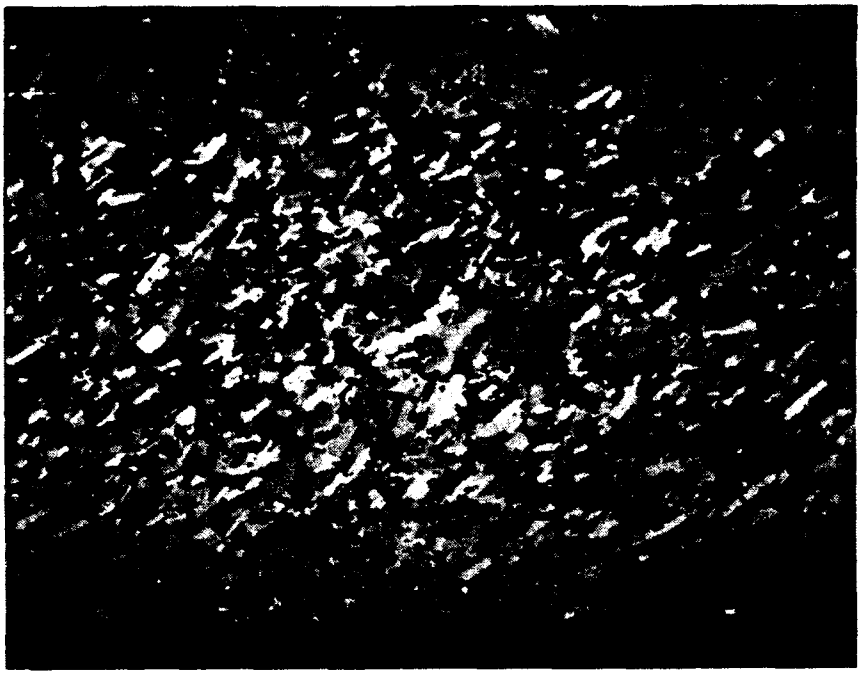

Fig. 7. The melt-textured longitudinal section of sample 10377-15B MT6 in polarized light showing finer grain size compared with the sample 10377-15B MT5 due to higher maximum temperature at 1006°C but the travelling speed was too fast for producing sufficient liquid phase. The sample shows very slight grain alignment (200X)

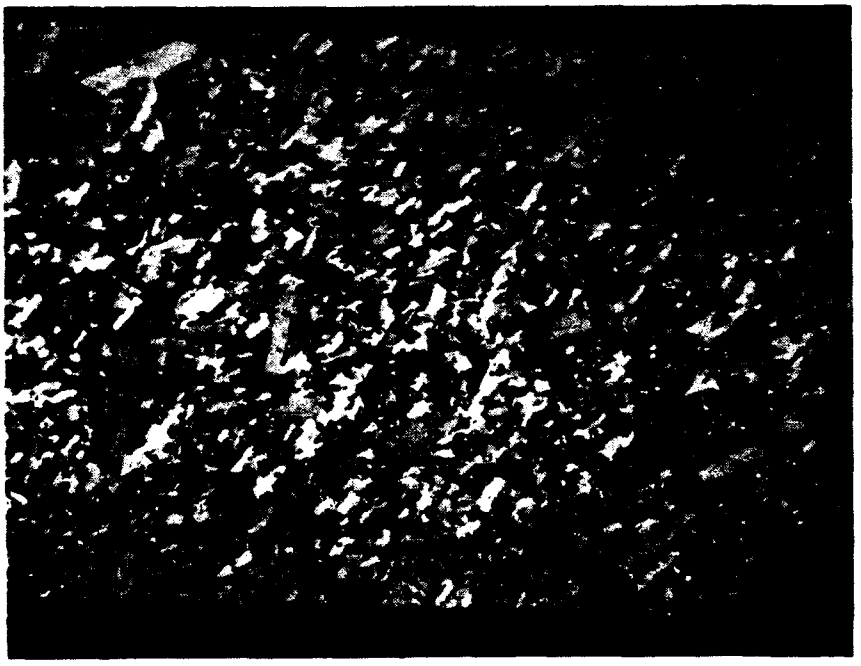

Fig. 8. The melt-textured longitudinal section in polarized light of sample 10337-15B MT8 showing slightly finer grain size than previous sample (200X)

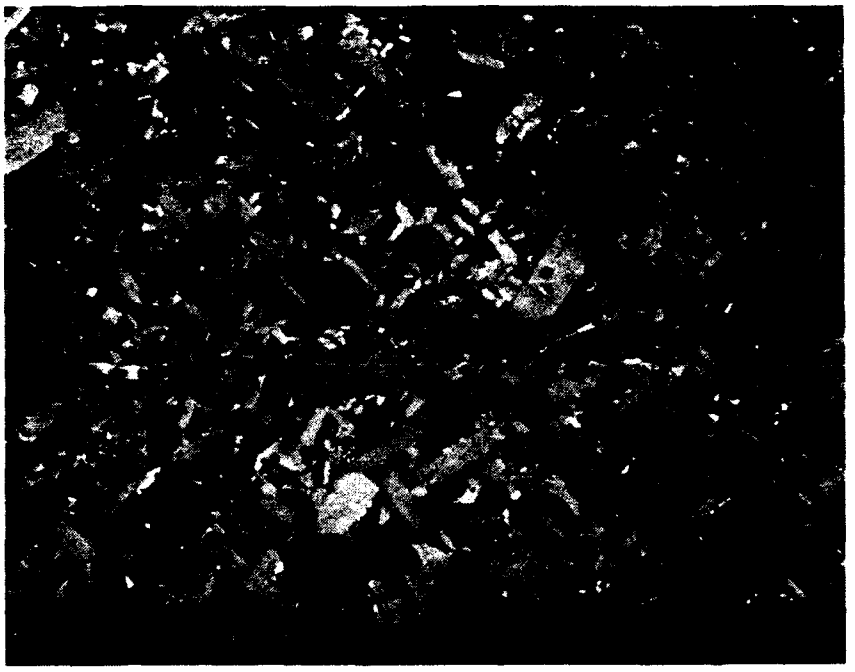

Fig. 9. The melt-textured longitudinal section of sample 10337-15B MT9 in polarized light showing excessive grain growth (200X)

the quartz tube, thus a portion of the rod received more infrared radiation than the other parts. Additionally, it was observed that the surface of all the melt-textured rods consisted of a thin layer of randomly oriented Y123 crystals. The layer consisted of fine-grained crystals but did not exhibit preferred orientation. There were also some porosity remained in the sample as shown in the electron micrograph [Fig. 3(d)]. It can be seen that the maximum temperature above 1050°C is very important for grain alignment.

Due to the drop off of the maximum temperature at the center of the unblocked sections, the infrared furnace was modified as mentioned earlier. By using this modified furnace, a second set of samples with diameter of 0.5 mm by 5 cm long were run with different speeds. The results are tabulated in Table 2.

The microstructure of this series of samples have not been examined, instead, the current densities of the sample were measured to find out whether the melt-texturing is successful or not. The field dependence of the current densities at 77K were also measured. The results are shown in Tables 3 through 5.

The current density of the tested samples is still low because the optimal heat treatment conditions have yet to be established. The melt-textured samples actually have lower J_c than the sample without melt-texturing (maximum J_c obtained without field is 1040 A/cm^2). However, the listed data in Tables 3 through 5 show that, even though the current density of the melt-textured sample MT005 was low, the field dependence has been considerably improved [J_c (H = 50 G)/J_c (H = 0) = 0.09].

TABLE 2
EXPERIMENTAL CONDITIONS FOR MELT-TEXTURING IN
IN FURNACE DESIGN IN FIG. 1(b)

Sample Size (mm)	Traveling Speed (cm/min)	Maximum Temperature (°C)	Maximum dT/dt (980° to 920°C) (-°C/min)	J_c (H = 0) (A/cm^2)
MT001	0.116	1085	-60	70
MT002	0.080	1082	-26	559
MT003	0.048	1085	-20	
MT004	0.017	1090	-7	
MT005	0.041	1105	-6	770
MT006	0.080	1118	-30	250
MT007	0.048	1110	-24	

TABLE 3
THE CURRENT DENSITY OF THE SAMPLE MT001
IN MAGNETIC FIELD

T (K)	H (G)	I (amp)	J_c (A/cm^2)
77.2	2.9	2.0	70
77.1	0.2	1.8	63
77.1	18.3	1.15	40
77.1	40.2	1.0	35
77.1	50.0	0.8	28
77.1	70.0	0.6	21
77.1	99.9	0.38	13
77.1	201.0	0.3	10

J_c (H = 50 G)/Jc (H = 0 G) = 0.40

TABLE 4
THE CURRENT DENSITY OF THE SAMPLE MT002
IN DIFFERENT MAGNETIC FIELD

T (K)	H (G)	I_c (amp)	J_c (A/cm^2)
67	0	6.8	883
76.38	0.05	4.3	559
77.07	28.0	1.7	221
77.04	48.0	1.15	149
77.04	76.55	0.6	78
77.00	98.67	0.42	53
77.00	148.2	0.235	31
77.00	200.00	0.1575	20
77.00	251.6	0.1175	15
77.00	350.0	0.1125	15

J_c (H = 48 G)/J_c (H = 0 G) = 0.27

TABLE 5
CURRENT DENSITY OF THE SAMPLE MT005
IN DIFFERENT FIELD

T (K)	H (G)	I (A)	J_c (A/cm^2)
75.72	0.39	4.8	772
75.32	18.84	4.6	739
75.15	49.66	2.8	450
75.03	104.49	1.25	201
74.95	202.2	0.62	100
74.83	304.5	0.42	66

J_c (H = 50 G)/J_c (H = 0 G) = 0.58